Appl. Comput. Harmon. Anal. 30 (2011) 231–242

Contents lists available at ScienceDirect

Applied and Computational Harmonic Analysis

www.elsevier.com/locate/acha

Analysis and detection of surface discontinuities using the 3D continuous shearlet transform

Kanghui Guo [a], Demetrio Labate [b,*,1]

[a] Department of Mathematics, Missouri State University, Springfield, MO 65804, USA
[b] Department of Mathematics, University of Houston, 651 Phillip G. Hoffman, Houston, TX 77204-3008, USA

ARTICLE INFO

Article history:
Received 16 February 2010
Revised 18 June 2010
Accepted 13 August 2010
Available online 20 August 2010
Communicated by Charles K. Chui

Keywords:
Analysis of singularities
Continuous wavelets
Curvelets
Directional wavelets
Edge detection
Shearlets
Wavelets

ABSTRACT

Directional multiscale transforms such as the shearlet transform have emerged in recent years for their ability to capture the geometrical information associated with the singularity sets of bivariate functions and distributions. One of the most striking features of the continuous shearlet transform is that it provides a very simple and precise geometrical characterization for the boundary curves of general planar regions. However, no specific results were known so far in higher dimensions, since the arguments used in dimension $n = 2$ do not directly carry over to the higher dimensional setting. In this paper, we extend this framework for the analysis of singularities to the 3-dimensional setting, and show that the 3-dimensional continuous shearlet transform precisely characterizes the boundary set of solid regions in $\mathbb{R}^3$ by identifying both its location and local orientation.

1. Introduction

Several methods have been recently introduced in the literature to overcome the limitations of the traditional wavelet transform in dealing with multidimensional data. In fact, while the continuous wavelet transform is able to identify the location of singularities of functions and distributions through its asymptotic behavior at fine scales [9,13], it lacks the ability to capture additional information about the geometry of the singularity set. This is a major disadvantage in imaging and other multidimensional applications such as those concerned with the identification of edges and surfaces of discontinuity.

The reason for this limitation is the intrinsic isotropic nature of the continuous wavelet transform. In contrast, the curvelet and shearlet transforms [1,11], two of the most successful generalizations of the wavelet approach recently introduced, offer a directional multiscale framework with the ability to precisely analyze functions and distributions not only in terms of locations and scales, but also according to their directional information. Indeed, the curvelet and shearlet transforms are compatible with the notion of *wavefront set* from microlocal analysis [14], which plays a major role in the study of propagation of singularities from PDEs [10]. For a distribution f, the wavefront set defines the location/direction pairs (x, θ) where local windowed versions of f are non-smooth in the θ direction and it was shown to correspond exactly to the points where the continuous curvelet and shearlet transforms have slow decay asymptotically at fine scales [1,11]. This point of view was further refined in [7,6] by providing a very precise characterization of the set of discontinuities of bivariate functions using the continuous shearlet transform $\mathcal{SH}_\psi$. This is defined as the mapping

* Corresponding author.
E-mail addresses: KanghuiGuo@MissouriState.edu (K. Guo), dlabate@math.uh.edu (D. Labate).
[1] D.L. acknowledges support by National Science Foundation grants DMS 0604561 and 0746778.

1063-5203/$ – see front matter
doi:10.1016/j.acha.2010.08.004

$$\mathcal{SH}_\psi : f \to \mathcal{SH}_\psi f(a,s,t) = \langle f, \psi_{a,s,t}\rangle,$$

taking a function $f \in L^2(\mathbb{R}^2)$ into the elements $\mathcal{SH}_\psi f(a,s,t)$ depending on the scale variable $a > 0$, the orientation variable $s \in \mathbb{R}$ and the locations $t \in \mathbb{R}^2$. Here the analyzing functions ψ_{ast} are well-localized waveforms associated with the variables a, s and t (the exact definition will be given below) and are especially designed to deal with the geometry of bivariate functions and distributions. In fact, let $B = \chi_S$, where $S \subset \mathbb{R}^2$ and its boundary ∂S is a piecewise smooth curve. It was shown in [6] (extending previous results in [7,11]) that both the location and the orientation of the boundary curve ∂S can be precisely identified from the asymptotic decay of $\mathcal{SH}_\psi B(a,s,p)$, as $a \to 0$. Specifically:

- If $p \notin \partial S$, then $|\mathcal{SH}_\psi B(a,s,p)|$ *decays rapidly*, as $a \to 0$, for each $s \in \mathbb{R}$. By *rapid decay*, we mean that, given any $N \in \mathbb{N}$, there is a $C_N > 0$ such that $|\mathcal{SH}_\psi B(a,s,p)| \leqslant Ca^N$, as $a \to 0$.
- If $p \in \partial S$ and ∂S is smooth near p, then $|\mathcal{SH}_\psi B(a,s,p)|$ *decays rapidly*, as $a \to 0$, for each $s \in \mathbb{R}$ unless $s = s_0$ is the normal orientation to ∂S at p. In this last case, $|\mathcal{SH}_\psi B(a,s_0,p)| \sim a^{\frac{3}{4}}$, as $a \to 0$.
- If p is a corner point of ∂S and $s = s_0$, $s = s_1$ are the normal orientations to ∂S at p, then $|\mathcal{SH}_\psi B(a,s_0,p)|$, $|\mathcal{SH}_\psi B(a,s_1,p)| \sim a^{\frac{3}{4}}$, as $a \to 0$. For all other orientations, the asymptotic decay of $|\mathcal{SH}_\psi B(a,s,p)|$ is faster (even if not necessarily "rapid").

These results provide the theoretical justification and the groundwork for improved numerical algorithms for edge analysis and detection, such as those introduced in [17], which further demonstrate the benefits of a directional multiscale transform with respect to the traditional wavelet approach. We refer to [3–5,12] for additional information about the discrete version of the shearlet transform and its numerical implementations.

The goal of this paper is to extend the results reported above to the 3-dimensional setting. This is motivated both by a mathematical desire for generalization and by the increasing need, in applications such as medical and seismic imaging, to identify and analyze surfaces of discontinuities and other distributed singularities in 3-dimensional data.

Indeed, the mathematical framework of the bivariate shearlet transform extends naturally to n dimensions since this transform arises from a square integrable representation of the shearlet group, and this group has a natural n-variate generalization, as shown in [2,11]. Unfortunately, while it is straightforward to define a 3-dimensional shearlet transform $\mathcal{SH}_\psi$, many of the techniques introduced in the previous work to study the asymptotic decay of $\mathcal{SH}_\psi$ at fine scales, in correspondence of singularities, do not carry over from the 2D to the 3D setting. This is due to the additional complexity of dealing with singularity sets which are defined on surfaces rather than along curves. Hence, to deal with the 3D problem, several new ideas and techniques have been developed in this paper to obtain appropriate estimates for the 3-dimensional continuous shearlet transform. Using these methods, we are able to show that, similarly to the 2-dimensional counterpart, if $B = \chi_C$, where $C \subset \mathbb{R}^3$ is a convex region with nonvanishing Gaussian curvature, then the 3-dimensional continuous shearlet transform of B has rapid asymptotic decay, at fine scales, for all locations except for the boundary surface ∂C, when the orientation variable corresponds to the normal direction to the surface.

The paper is organized as follows. The definition of the shearlet transform, including the properties which are needed for the arguments used in the proofs of this paper, are given in Section 2. The main theorem and the other results which are needed for its proof are given in Section 3.

2. The shearlet transform

We recall the basic properties of the continuous shearlet transform, which was originally introduced in [11]. Consider the subspace of $L^2(\mathbb{R}^3)$ given by $L^2(C^{(1)})^\vee = \{f \in L^2(\mathbb{R}^3)\colon \operatorname{supp}\hat f \subset C^{(1)}\}$, where $C^{(1)}$ is the "horizontal cone" in the frequency plane:

$$C^{(1)} = \left\{(\xi_1,\xi_2,\xi_3) \in \mathbb{R}^3\colon |\xi_1| \geqslant 2,\ \left|\frac{\xi_2}{\xi_1}\right| \leqslant 1 \text{ and } \left|\frac{\xi_3}{\xi_1}\right| \leqslant 1\right\}.$$

The following proposition, which is a simple generalization of a result from [11], provides sufficient conditions on the function ψ for obtaining a reproducing system of continuous shearlets on $L^2(C^{(1)})^\vee$.

Proposition 2.1. *Consider the shearlet group $\Lambda^{(1)} = \{(M_{as_1s_2}, p)\colon 0 \leqslant a \leqslant \frac{1}{4}, -\frac{3}{2} \leqslant s_1 \leqslant \frac{3}{2}, -\frac{3}{2} \leqslant s_2 \leqslant \frac{3}{2}, p \in \mathbb{R}^2\}$, where*

$$M_{as_1s_2} = \begin{pmatrix} a & -a^{1/2}s_1 & -a^{1/2}s_2 \\ 0 & a^{1/2} & 0 \\ 0 & 0 & a^{1/2} \end{pmatrix}.$$

For $\xi = (\xi_1,\xi_2,\xi_3) \in \mathbb{R}^3$, $\xi_1 \neq 0$, let $\psi^{(1)}$ be defined by

$$\hat\psi^{(1)}(\xi) = \hat\psi^{(1)}(\xi_1,\xi_2,\xi_3) = \hat\psi_1(\xi_1)\hat\psi_2\left(\frac{\xi_2}{\xi_1}\right), \hat\psi_2\left(\frac{\xi_3}{\xi_1}\right),$$

where:

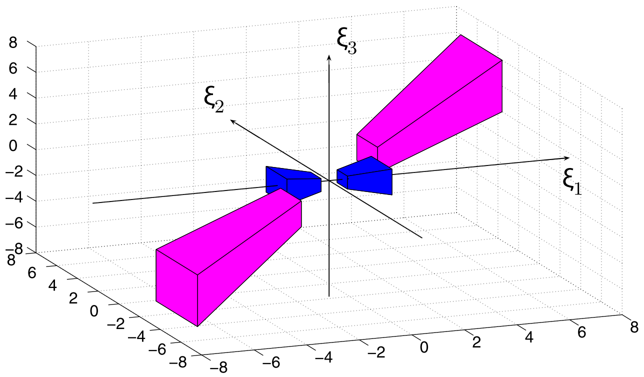

Fig. 1. Support of the shearlet $\hat{\psi}^{(1)}_{as_1s_2p}$, in the frequency domain, for $a = 1/4$, $s_1 = s_2 = 0$ (darker [blue] region) and for $a = 1/16$, $s_1 = 0.7, s_2 = 0.5$ (lighter [magenta] region). (For interpretation of colors in this figure, the reader is referred to the web version of this article.)

(i) $\psi_1 \in L^2(\mathbb{R})$ *satisfies the Calderòn condition*

$$\int_0^\infty \left|\hat{\psi}_1(a\xi)\right|^2 \frac{da}{a} = 1 \quad \text{for a.e. } \xi \in \mathbb{R}, \tag{1}$$

and $\operatorname{supp} \hat{\psi}_1 \subset [-2, -\frac{1}{2}] \cup [\frac{1}{2}, 2]$;

(ii) $\|\psi_2\|_{L^2} = 1$ *and* $\operatorname{supp} \hat{\psi}_2 \subset [-\frac{\sqrt{2}}{4}, \frac{\sqrt{2}}{4}]$.

Let $\psi^{(1)}_{as_1s_2p}(x) = |\det M_{as_1s_2}|^{-\frac{1}{2}} \psi^{(1)}(M^{-1}_{as_1s_2}(x-p))$. *Then, for all* $f \in L^2(C^{(1)})^\vee$,

$$f(x) = \int_{\mathbb{R}^3} \int_{-\frac{3}{2}}^{\frac{3}{2}} \int_{-\frac{3}{2}}^{\frac{3}{2}} \int_0^{\frac{1}{4}} \langle f, \psi^{(1)}_{as_1s_2p}\rangle \psi^{(1)}_{as_1s_2p}(x) \frac{da}{a^4}\, ds_1\, ds_2\, dp,$$

with convergence in the L^2 *sense.*

If the assumptions of Proposition 2.1 are satisfied, we say that the functions

$$\Psi^{(1)} = \left\{\psi^{(1)}_{as_1s_2p}\colon 0 \leqslant a \leqslant \frac{1}{4},\ -\frac{3}{2} \leqslant s_1 \leqslant \frac{3}{2},\ -\frac{3}{2} \leqslant s_2 \leqslant \frac{3}{2},\ p \in \mathbb{R}^2\right\} \tag{2}$$

are *continuous shearlets* for $L^2(C^{(1)})^\vee$ and that the corresponding mapping from $f \in L^2(C^{(1)})^\vee$ into $\mathcal{SH}^{(1)} f(a, s_1, s_2, p) = \langle f, \psi^{(1)}_{as_1s_2p}\rangle$ is the *continuous shearlet transform* on $L^2(C^{(1)})^\vee$ with respect to $\Lambda^{(1)}$. The index label (1) used in the notation of the shearlet system $\Psi^{(1)}$ (and the corresponding shearlet transform) indicates that the system in the expression (2) has frequency support in the cone $C^{(1)} \subset \mathbb{R}^3$; other shearlet systems will be defined below with support in two other complementary cone regions.

Observe that, in the frequency domain, a shearlet $\psi^{(1)}_{as_1s_2p} \in \Psi^{(1)}$ has the form

$$\hat{\psi}^{(1)}_{as_1s_2p}(\xi_1, \xi_2, \xi_3) = a\hat{\psi}_1(a\xi_1)\hat{\psi}_2\left(a^{-\frac{1}{2}}\left(\frac{\xi_2}{\xi_1} - s_1\right)\right)\hat{\psi}_2\left(a^{-\frac{1}{2}}\left(\frac{\xi_3}{\xi_1} - s_2\right)\right)e^{-2\pi i\xi p}.$$

Thus, the functions $\hat{\psi}^{(1)}_{as_1s_2p}$ have supports in the sets

$$\left\{(\xi_1, \xi_2, \xi_3)\colon \xi_1 \in \left[-\frac{2}{a}, -\frac{1}{2a}\right] \cup \left[\frac{1}{2a}, \frac{2}{a}\right],\ \left|\frac{\xi_2}{\xi_1} - s_1\right| \leqslant \frac{\sqrt{2}}{4}a^{\frac{1}{2}},\ \left|\frac{\xi_3}{\xi_1} - s_2\right| \leqslant \frac{\sqrt{2}}{4}a^{\frac{1}{2}}\right\}.$$

That is, the frequency support of each function $\hat{\psi}^{(1)}_{as_1s_2p}$ is a pair of hyper-trapezoids, symmetric with respect to the origin, with orientation determined by the slope parameters s_1, s_2. The support region becomes increasingly elongated as $a \to 0$. Some examples of these support regions are illustrated in Fig. 1.

There are a variety of examples of functions ψ_1 and ψ_2 satisfying the assumptions of Proposition 2.1. In particular, one can find a number of such examples with the additional property that $\hat{\psi}_1, \hat{\psi}_2 \in C_0^\infty$ [4,11]. For the kind of applications which will be described in this paper, some further additional properties are needed. In particular, we will require that $\hat{\psi}_1$

is a smooth odd function, and that $\hat{\psi}_2$ is an even smooth function which is decreasing on $[0, \frac{\sqrt{2}}{4})$. Hence, to summarize, in the following we will assume that

$$\hat{\psi}_1\colon\quad C_0^\infty,\ \operatorname{supp}\hat{\psi}_1 \subset \left[-2, -\frac{1}{2}\right] \cup \left[\frac{1}{2}, 2\right],\ \text{odd and it satisfies (1);} \tag{3}$$

$$\hat{\psi}_2\colon\quad C_0^\infty,\ \operatorname{supp}\hat{\psi}_2 \subset \left[-\frac{\sqrt{2}}{4}, \frac{\sqrt{2}}{4}\right],\ \text{even, decreasing in } \left[0, \frac{\sqrt{2}}{4}\right),\ \|\psi_2\| = 1. \tag{4}$$

Notice that the shearlet system $\Psi^{(1)}$, given by (2), generates a reproducing system for only a proper subspace of $L^2(\mathbb{R}^3)$. To extend this construction and the corresponding continuous shearlet transform to deal with the whole space $L^2(\mathbb{R}^3)$, we can introduce similar systems defined on the complementary cone regions. Namely, let

$$C^{(2)} = \left\{(\xi_1, \xi_2, \xi_3) \in \mathbb{R}^3\colon\ |\xi_2| \geqslant 2,\ \left|\frac{\xi_2}{\xi_1}\right| > 1,\ \left|\frac{\xi_3}{\xi_1}\right| \leqslant 1\right\}$$

and

$$C^{(3)} = \left\{(\xi_1, \xi_2, \xi_3) \in \mathbb{R}^3\colon\ |\xi_2| \geqslant 2,\ \left|\frac{\xi_2}{\xi_1}\right| \leqslant 1,\ \left|\frac{\xi_3}{\xi_1}\right| > 1\right\},$$

so that $\bigcup_{i=1}^3 C^{(i)} = \mathbb{R}^3$, and, for $i = 2, 3$, define the shearlet groups

$$\Lambda^{(i)} = \left\{(M_{as_1s_2}, p)^{(i)}\colon\ 0 \leqslant a \leqslant \frac{1}{4},\ -\frac{3}{2} \leqslant s_1 \leqslant \frac{3}{2},\ -\frac{3}{2} \leqslant s_2 \leqslant \frac{3}{2},\ p \in \mathbb{R}^2\right\},$$

where

$$M_{as_1s_2}^{(2)} = \begin{pmatrix} a^{1/2} & 0 & 0 \\ -a^{1/2}s_1 & a & -a^{1/2}s_2 \\ 0 & 0 & a^{1/2} \end{pmatrix}, \qquad M_{as_1s_2}^{(3)} = \begin{pmatrix} a^{1/2} & 0 & 0 \\ 0 & a^{1/2} & 0 \\ -a^{1/2}s_1 & -a^{1/2}s_2 & a \end{pmatrix}.$$

Next, let

$$\hat{\psi}^{(2)}(\xi) = \hat{\psi}^{(2)}(\xi_1, \xi_2, \xi_3) = \hat{\psi}_1(\xi_2)\hat{\psi}_2\left(\frac{\xi_1}{\xi_2}\right)\psi_2\left(\frac{\xi_3}{\xi_2}\right),$$
$$\hat{\psi}^{(3)}(\xi) = \hat{\psi}^{(2)}(\xi_1, \xi_2, \xi_3) = \hat{\psi}_1(\xi_3)\hat{\psi}_2\left(\frac{\xi_1}{\xi_3}\right)\psi_2\left(\frac{\xi_2}{\xi_3}\right),$$

where $\hat{\psi}_1$, $\hat{\psi}_2$ satisfy the same assumptions as in Proposition 2.1, and denote

$$\psi_{as_1s_2p}^{(i)} = \left|\det M_{as_1s_2}^{(i)}\right|^{-\frac{1}{2}} \psi^{(i)}\left(\left(M_{as_1s_2}^{(i)}\right)^{-1}(x - p)\right), \quad \text{for } i = 2, 3.$$

Then an argument similar to the one from Proposition 2.1 shows that, for $i = 2, 3$, the functions

$$\Psi^{(i)} = \left\{\psi_{as_12_2p}^{(i)}\colon\ 0 \leqslant a \leqslant \frac{1}{4},\ -\frac{3}{2} \leqslant s_1 \leqslant \frac{3}{2},\ -\frac{3}{2} \leqslant s_1 \leqslant \frac{3}{2},\ p \in \mathbb{R}^2\right\}$$

are continuous shearlets for $L^2(C^{(i)})^\vee$. Also, for $i = 2, 3$, the transforms $\mathcal{SH}_\psi^{(i)} f(a, s_1, s_2, p) = \langle f, \psi_{as_1s_2p}^{(i)}\rangle$ are the continuous shearlet transform on $L^2(C^{(i)})^\vee$ with respect to $\Lambda^{(i)}$. Finally, by introducing an appropriate smooth, bandlimited window function W, we can represent the functions with frequency support on the set $[-2, 2]^3$ as

$$f = \int_{\mathbb{R}^3} \langle f, W_p\rangle W_p\, dp,$$

where $W_p(x) = W(x - p)$. As a result, we can represent any function $f \in L^2(\mathbb{R}^3)$ with respect to the full system of shearlets, which consists of the systems $\bigcup_{i=1}^3 \Psi^{(i)}$ together with the coarse-scale isotropic functions W_p. The decomposition we have described generalizes a similar decomposition originally introduced in [11], for dimension $n = 2$.

Notice that, for the purposes of this paper, it is only the behavior of the fine-scale shearlets that matters. Indeed, the continuous shearlet transforms $\mathcal{SH}_\psi^{(i)}$, $i = 1, 2, 3$, will be applied at fine scales ($a \to 0$) to resolve and precisely describe the boundaries of certain solid regions. Since the behavior of these transforms is essentially the same on each cone domain $C^{(i)}$, in the following sections, without of loss of generality, we will only consider the continuous shearlet transform $\mathcal{SH}_\psi^{(1)}$. For simplicity of notation, we will drop the upperscript (1) in the following.

3. Analysis of singularities

As described above, the continuous shearlet transform is especially designed to deal with directional information at various scales and was proved particularly effective to characterize the boundary curves of planar regions [7,6].

To illustrate the properties of the continuous shearlet transform in dimension $n = 3$, let us start by considering the most basic model of surface discontinuity, which is given by the 3-dimensional Heaviside function $H(x_1, x_2, x_3) = \chi_{x_1>0}(x_1, x_2, x_3)$. We have the following simple characterization.

- If $p = (p_1, p_2, p_3)$, with $p_1 \neq 0$, then

$$\lim_{a\to 0^+} a^{-N} \mathcal{SH}_\psi H(a, s_1, s_2, p) = 0, \quad \text{for all } N > 0.$$

- If $\bar{s}_1 \neq 0$ or $\bar{s}_2 \neq 0$, then

$$\lim_{a\to 0^+} a^{-N} \mathcal{SH}_\psi H(a, \bar{s}_1, \bar{s}_2, p) = 0, \quad \text{for all } N > 0.$$

- If $p_1 = s_1 = s_2 = 0$, then

$$\lim_{a\to 0^+} a^{-1} \mathcal{SH}_\psi H(a, 0, 0, p) \neq 0.$$

That is, the continuous shearlet transform of H has rapid asymptotic decay as $a \to 0$, unless p is on the plane $x_1 = 0$ and s_1, s_2 correspond to the normal direction to the plane.

To justify this result, notice that $\frac{\partial}{\partial x_1} H = \delta_1$, where δ_1 is the delta distribution defined by

$$\langle \delta_1, \phi\rangle = \int\int \phi(0, x_2, x_3)\, dx_1\, dx_2,$$

where ϕ is a function in the Schwartz class $\mathcal{S}(\mathbb{R}^3)$ (notice that here we use the notation of the inner product $\langle,\rangle$ to denote the functional on $\mathcal{S}$). Hence

$$\hat{H}(\xi_1, \xi_2, \xi_3) = (2\pi i \xi_1)^{-1} \hat{\delta}_1(\xi_1, \xi_2, \xi_3),$$

where $\hat{\delta}_1$ is the distribution obeying

$$\langle \hat{\delta}_1, \hat{\phi}\rangle = \int\int \hat{\phi}(\xi_1, 0, 0)\, d\xi_1.$$

The continuous shearlet transform of H can now be expressed as

$$\begin{aligned}
\mathcal{SH}_\psi H(a, s_1, s_2, p) &= \langle H, \psi_{as_1s_2p}\rangle \\
&= \int_{\mathbb{R}^3} (2\pi i \xi_1)^{-1} \hat{\delta}_1(\xi) \overline{\hat{\psi}_{as_1s_2p}}(\xi)\, d\xi \\
&= \int_{\mathbb{R}} (2\pi i \xi_1)^{-1} \overline{\hat{\psi}_{as_1s_2p}}(\xi_1, 0, 0)\, d\xi_1 \\
&= \int_{\mathbb{R}} \frac{a}{2\pi i \xi_1} \overline{\hat{\psi}_1}(a\xi_1) \overline{\hat{\psi}_2}\big(a^{-\frac{1}{2}} s_1\big) \overline{\hat{\psi}_2}\big(a^{-\frac{1}{2}} s_2\big) e^{2\pi i \xi_1 p_1}\, d\xi_1 \\
&= \frac{a}{2\pi i} \overline{\hat{\psi}_2}\big(a^{-\frac{1}{2}} s_1\big) \overline{\hat{\psi}_2}\big(a^{-\frac{1}{2}} s_2\big) \int_{\mathbb{R}} \overline{\hat{\psi}_1}(u) e^{2\pi i u \frac{p_1}{a}} \frac{du}{u},
\end{aligned}$$

where p_1 is the first component of $p \in \mathbb{R}^3$.

Notice that, by the properties of ψ_1, the function $\tilde{\psi}_1(v) = \int_{\mathbb{R}} \overline{\hat{\psi}_1}(u) e^{2\pi i u v} \frac{du}{u}$ decays rapidly, asymptotically, as $v \to \infty$. Hence, if $p_1 \neq 0$, it follows that $\tilde{\psi}_1(\frac{p_1}{a})$ decays rapidly, asymptotically, as $a \to 0$, and, as a result, $\mathcal{SH}_\psi H(a, s_1, s_2, p)$ also has rapid decay as $a \to 0$. Similarly, by the support conditions of $\hat{\psi}_2$, if $s_1 \neq 0$ or $s_2 \neq 0$, it follows that the function $\hat{\psi}_2(a^{-\frac{1}{2}} s_1)$ or the function $\hat{\psi}_2(a^{-\frac{1}{2}} s_2)$ approaches 0 as $a \to 0$. Finally, if $p_1 = s_1 = s_2 = 0$, then

$$a^{-1} \mathcal{SH}_\psi H\big(a, 0, 0, (0, p_2, p_3)\big) = \frac{1}{2\pi i} \big(\overline{\hat{\psi}_2}(0)\big)^2 \int_{\mathbb{R}} \overline{\hat{\psi}_1}(u) \frac{du}{u} \neq 0.$$

In fact, using an appropriate change of variables, the result shown above can be extended to deal with discontinuities along planes with arbitrary orientations. Namely, if the plane of discontinuity has normal vector $(\sin\phi\cos\theta, \sin\phi\sin\theta, \cos\phi)$, then the continuous shearlet transform has rapid decay, except for p on the plane and (s_1, s_2) satisfying:

$$s_1 = \tan\theta, \qquad s_2 = \cot\phi\sec\theta. \tag{5}$$

Notice that the ideas of the arguments used above are similar to the 2-dimensional approach used in [1,11].

If the discontinuity occurs along a more general surface, the analysis becomes more involved and cannot be obtained by a direct extension of the 2-dimensional arguments used in any of the references mentioned above. However, using a novel approach, in the following we show that, for functions with discontinuities along smooth surfaces, the behavior of their continuous shearlet transform is consistent with the situation of the Heaviside function. Specifically, consider the functions $B = \chi_\Omega$, where Ω is a subset of $\mathbb{R}^3$ whose boundary is smooth and has nonzero Gaussian curvature. The following theorem shows that the continuous shearlet transform of B, denoted by $\mathcal{SH}_\psi B(a, s_1, s_2, p)$, has rapid asymptotic decay as $a \to 0$ for all locations $p \in \mathbb{R}^3$, except when p is on the boundary of Ω and the orientation variables s_1, s_2 correspond to normal direction with respect to the boundary surface. The statement given by this theorem is the analogue the corresponding 2D result found in [7].

Theorem 3.1. *Let Ω be a region in $\mathbb{R}^3$ and denote its boundary by $\partial\Omega$. Assume that $\partial\Omega$ is a C^∞ smooth surface and has positive Gaussian curvature at every point. Set $B = \chi_\Omega$.*

(i) *If $p \notin \partial\Omega$ then*

$$\lim_{a\to 0^+} a^{-N}\mathcal{SH}_\psi B(a, s_1, s_2, p) = 0, \quad \textit{for all } N > 0.$$

(ii) *If $p \in \partial\Omega$ and (s_1, s_2) does not correspond to the normal direction of $\partial\Omega$ at p then*

$$\lim_{a\to 0^+} a^{-N}\mathcal{SH}_\psi B(a, s_1, s_2, p) = 0, \quad \textit{for all } N > 0.$$

(iii) *If $p \in \partial\Omega$ and $(s_1, s_2) = (\bar{s}_1, \bar{s}_2)$ corresponds to the normal direction of $\partial\Omega$ at p, then*

$$\lim_{a\to 0^+} a^{-1}\mathcal{SH}_\psi B(a, \bar{s}_1, \bar{s}_2, p) \neq 0.$$

It is useful to observe that, if the normal orientation is expressed as the vector $n(\theta, \phi) = (\sin\phi\cos\theta, \sin\phi\sin\theta, \cos\phi)$ in spherical coordinates, then the values of (s_1, s_2) for the normal orientation are given by (5). Also notice that, if the boundary curve $\partial\Omega$ is not C^∞-regular but only C^M-regular, for some $M \in N$, then Theorem 3.1 is still true with the difference that statements (i) and (ii) will not hold for all $N > 0$, but only for all $0 < N < N^*(M)$, where $N^*(M)$ is a number dependent on M.

The proof of Theorem 3.1 will be given in Section 3.2, after some preparation which will be described below.

3.1. Useful lemmata

Let $\Omega \subset \mathbb{R}^3$ be a solid region whose boundary surface $S = \partial\Omega$ is smooth with nonvanishing Gaussian curvature and let $B = \chi_\Omega$. By the divergence theorem, we can write the Fourier transform of B as

$$\hat{B}(\xi) = \hat{\chi}_S(\xi) = -\frac{1}{2\pi i|\xi|^2}\int_S e^{-2\pi i\xi x}\xi\cdot\vec{n}(x)\,d\sigma(x), \tag{6}$$

where $\vec{n}$ is the normal vector to S at x (we follow here the approach used in [8]).

By representing $\xi \in \mathbb{R}^3$ using spherical coordinates as $\xi = \rho\Theta$, where $\rho \in \mathbb{R}^+$ and $\Theta = \Theta(\phi, \theta) = (\sin\phi\cos\theta, \sin\phi\sin\theta, \cos\phi)$ with $0 \leqslant \phi \leqslant \pi$ and $0 \leqslant \theta \leqslant 2\pi$, expression (6) can be written as

$$\hat{B}(\rho, \phi, \theta) = -\frac{1}{2\pi i\rho}\int_S e^{-2\pi i\rho\Theta\cdot x}\Theta\cdot\vec{n}(x)\,d\sigma(x). \tag{7}$$

For an $\epsilon > 0$, let $B_\epsilon(p)$ be the ball with radius ϵ and center p and let $P_\epsilon(p) = S \cap B_\epsilon(p)$. Hence we can break up the integral (7) as

$$\hat{B}(\rho, \phi, \theta) = T_1(\rho, \phi, \theta) + T_2(\rho, \phi, \theta),$$

where

$$T_1(\rho,\phi,\theta) = -\frac{1}{2\pi i\rho} \int\limits_{P_\epsilon(p)} e^{-2\pi i\rho\Theta\cdot x}\Theta \cdot \vec{n}(x)\, d\sigma(x),$$

$$T_2(\rho,\phi,\theta) = -\frac{1}{2\pi i\rho} \int\limits_{S\setminus P_\epsilon(p)} e^{-2\pi i\rho\Theta\cdot x}\Theta \cdot \vec{n}(x)\, d\sigma(x).$$

It follows that

$$\mathcal{SH}_\psi B(a,s_1,s_2,p) = \langle B, \psi_{as_1s_2p}\rangle = I_1(a,s_1,s_2,p) + I_2(a,s_1,s_2,p),$$

where, for $i = 1, 2$, we have

$$I_i(a,s_1,s_2,p) = \int_0^{2\pi}\int_0^{\pi}\int_0^{\infty} T_i(\rho,\phi,\theta)\overline{\hat{\psi}_{as_1s_2p}}(\rho,\phi,\theta)\rho^2 \sin\phi\, d\rho\, d\phi\, d\theta. \tag{8}$$

The following lemma shows that the asymptotic decay of the shearlet transform $\mathcal{SH}_\psi B(a,s_1,s_2,p)$, as $a \to 0$, is only determined by the values of the boundary surface S which are "close" to the location variable p.

Lemma 3.1. *For any positive integer N, there is a constant $C_N > 0$ such that*

$$\left|I_2(a,s_1,s_2,p)\right| \leqslant C_N a^N,$$

asymptotically as $a \to 0$, uniformly for all $s_1, s_2 \in [-\frac{3}{2}, \frac{3}{2}]$.

Proof. By direct computation, we have that:

$$\begin{aligned}
-2\pi i I_2(a,s_1,s_2,p) &= \int\limits_{S\setminus P_\epsilon(p)} \int_0^{2\pi}\int_0^{\pi}\int_0^{\infty} e^{-2\pi i\rho\Theta\cdot x}\Theta\cdot\vec{n}(x)\overline{\hat{\psi}_{as_1s_2p}}(\rho,\phi,\theta)\rho\sin\phi\, d\rho\, d\phi\, d\theta\, d\sigma(x) \\
&= a \int\limits_{S\setminus P_\epsilon(p)} \int_0^{2\pi}\int_0^{\pi}\int_0^{\infty} \hat{\psi}_1(a\rho\sin\phi\cos\theta)\hat{\psi}_2\big(a^{-\frac{1}{2}}(\tan\theta - s_1)\big) \\
&\quad \times \hat{\psi}_2\big(a^{-\frac{1}{2}}(\cot\phi\sec\theta - s_2)\big)e^{2\pi i\rho\Theta(\phi,\theta)\cdot(p-x)}\Theta\cdot\vec{n}(x)\rho\sin\phi\, d\rho\, d\phi\, d\theta\, d\sigma(x) \\
&= \frac{1}{a} \int\limits_{S\setminus P_\epsilon(p)} \int_0^{2\pi}\int_0^{\pi}\int_0^{\infty} \hat{\psi}_1(\rho\sin\phi\cos\theta)\hat{\psi}_2\big(a^{-\frac{1}{2}}(\tan\theta - s_1)\big) \\
&\quad \times \hat{\psi}_2\big(a^{-\frac{1}{2}}(\cot\phi\sec\theta - s_2)\big)e^{2\pi i\frac{\rho}{a}\Theta(\phi,\theta)\cdot(p-x)}\Theta\cdot\vec{n}(x)\rho\sin\phi\, d\rho\, d\phi\, d\theta\, d\sigma(x).
\end{aligned}$$

Notice that, by assumption, there exists an $\epsilon > 0$ such that $\|p - x\| \geqslant \epsilon$ for all $x \in S \setminus P_\epsilon(p)$. Let $s_1 = \tan\theta_0$ with $|\theta_0| < \frac{\pi}{2}$ and $s_2 = \cot\phi_0\sec\theta_0$ with $|\phi_0 - \frac{\pi}{2}| < \frac{\pi}{2}$. By the support condition of $\hat{\psi}_2$, it follows that, for a near 0, θ is away from $\frac{\pi}{2}$ or $\frac{3\pi}{2}$ and ϕ is away from 0 or π. Let J be the set of these θ and ϕ. It is easy to see that $\{\Theta(\phi,\theta), \Theta_\phi(\phi,\theta), \Theta_\theta(\phi,\theta)\}$ form a basis for $\mathbb{R}^3$ for $(\phi,\theta) \in J$. It follows that there is a constant $C_p > 0$ such that $|\Theta(\phi,\theta)\cdot(p-x)| + |\Theta_\phi(\phi,\theta)\cdot(p-x)| + |\Theta_\theta(\phi,\theta)\cdot(p-x)| \geqslant C_p$, where C_p is independent of $(\phi,\theta) \in J$, and $x \in S \setminus P_\epsilon(p)$.

Define

$$J_1 = \left\{(\phi,\theta)\colon \inf_{x\in S\setminus P_\epsilon(p)} \left|\Theta(\phi,\theta)\cdot(p-x)\right| \geqslant \frac{C_p}{3}\right\},$$

$$J_2 = \left\{(\phi,\theta)\colon \inf_{x\in S\setminus P_\epsilon(p)} \left|\Theta_\phi(\phi,\theta)\cdot(p-x)\right| \geqslant \frac{C_p}{3}\right\},$$

$$J_3 = \left\{(\phi,\theta)\colon \inf_{x\in S\setminus P_\epsilon(p)} \left|\Theta_\theta(\phi,\theta)\cdot(p-x)\right| \geqslant \frac{C_p}{3}\right\}.$$

We can express integral I_2 as a sum of three integrals corresponding to J_1, J_2, and J_3 respectively. On J_1, we integrate by parts with respect to the variable ρ; on J_2 we integrate by parts with respect to the variable ϕ, and on J_3 we integrate by parts with respect to the variable θ. Doing this repeatedly, it yields that, for any positive integer n, $|I_2| \leqslant C_n a^{\frac{n}{2}}$. This finishes the proof. □

It is useful to recall the definition of *nondegenerate critical point*, which will be needed in the next lemma.

Definition 3.1. Let $\Phi : \mathbb{R}^2 \to \mathbb{R}$ be a smooth function and suppose that Φ has a critical point at u_0, that is, $\Delta\Phi(u_0) = (0,0)$. If the matrix $A_\Phi(u_0) = (\Phi_{u_i u_j}(u_0))_{1\leqslant i,j\leqslant 2}$ is invertible, then u_0 is a *nondegenerate critical point* of Φ.

The following result is a special 2-dimensional case of the method of stationary phase, which can be found in [15, Prop. 6, p. 344].

Lemma 3.2. *Let $\Phi : \mathbb{R}^2 \to \mathbb{R}$ be a C^∞ function which has a nondegenerate critical point at $u_0 \in \mathbb{R}^2$. If ψ is supported in a sufficiently small neighborhood of u_0, then*

$$I(\lambda) = \int_{\mathbb{R}^2} e^{i\lambda\Phi(u)}\psi(u)\,du = e^{i\lambda\Phi(u_0)}\big[a_0\lambda^{-1} + O\big(\lambda^{-2}\big)\big],$$

as $\lambda \to \infty$, where

$$a_0 = 2\pi\,\psi(u_0)\big(-\det\big(A_\Phi(u_0)\big)\big)^{-\frac{1}{2}}.$$

We also recall the following formulation of the Implicit Function Theorem for $n = 2$.

Lemma 3.3. *Let $t = (t_1, t_2) \in \mathbb{R}^2$, $u = (u_1, u_2) \in \mathbb{R}^2$. Suppose that $F(t,u) = (F_1(t,u), F_2(t,u))$ is a C^∞ function from $T \times U$ to $\mathbb{R}^2$, where T and U are open sets in $\mathbb{R}^2$. Assume that, for some $t_0 \in T$ and $u_0 \in U$, we have $F(t_0,u_0) = (0,0)$ and that Jacobian of F satisfies: $J_u(F)(t_0,u_0) \neq 0$. We then have the following:*

(i) *there exists an open set $T_0 \subset T$ with $t_0 \in T_0$ and a smooth function $u = u(t)$ such that $F(t,u(t)) = (0,0)$ for all $t \in T_0$;*
(ii) *for $j = 1,2$, $u_{t_j} = \frac{1}{J_u(F)(t,u)}(F_{2t_j}F_{1u_2} - F_{1t_j}F_{2u_2}, F_{1t_j}F_{2u_1} - F_{2t_j}F_{1u_1})$.*

The following lemma is a generalization of Lemma 4.4 in [6].

Lemma 3.4. *For $\alpha \in [0,2\pi)$, $y > 0$, let*

$$g(\alpha,y) = 2y\int_0^1 \hat{\psi}_2(r\cos\alpha)\hat{\psi}_2(r\sin\alpha)\sin\big(\pi y r^2\big)r\,dr,$$

where ψ_2 satisfies the assumptions given by (4). Then $g(\alpha,y) > 0$.

Proof. Let $f_\alpha(r) = \hat{\psi}_2(r\cos\alpha)\hat{\psi}_2(r\sin\alpha)$. By the assumption on $\hat{\psi}_2$, it follows that, for each $\alpha \in [0,2\pi)$, $f_\alpha(r)$ is decreasing on $[0,\frac{1}{2})$, that $f_\alpha(0) > 0$ and $f_\alpha(r) = 0$ for $r \geqslant \frac{1}{2}$. We can write $g(\alpha,y)$ as

$$g(\alpha,y) = \int_0^y f_\alpha\left(\sqrt{\frac{v}{y}}\right)\sin(\pi v)\,dv.$$

If $y \leqslant 1$, it is trivial to see that $g(\alpha,y) > 0$ since $f_\alpha(0) > 0$, $f_\alpha(r) \geqslant 0$ on $[0,1]$ and $\sin(\pi x) > 0$ on $(0,1)$. Now consider the case where $1 < y \leqslant 2$. Since $f_\alpha(r)$ is decreasing on $(0,\frac{1}{2})$ and $\hat{\psi}_2(r) = 0$ for $r \geqslant \frac{1}{2}$, it follows that

$$\begin{aligned}
g(\alpha,y) &= \int_0^1 f_\alpha\left(\sqrt{\frac{v}{y}}\right)\sin(\pi v)\,dv + \int_1^y f_\alpha\left(\sqrt{\frac{v}{y}}\right)\sin(\pi v)\,dv \\
&= \int_0^1 f_\alpha\left(\sqrt{\frac{v}{y}}\right)\sin(\pi v)\,dv - \int_0^{y-1} f_\alpha\left(\sqrt{\frac{v+1}{y}}\right)\sin(\pi v)\,dv \\
&\geqslant \int_0^1 \left(f_\alpha\left(\sqrt{\frac{v}{y}}\right) - f_\alpha\left(\sqrt{\frac{v+1}{y}}\right)\right)\sin(\pi v)\,dv > 0.
\end{aligned}$$

For $y > 2$, one can find $k \geqslant 1$ and $0 < \zeta \leqslant 2$ such that $y = 2k + \zeta$. In this case, we have

$$g(\alpha, y) = \int_0^{2k} f_\alpha\left(\sqrt{\frac{v}{y}}\right)\sin(\pi v)\,dv + \int_{2k}^{y} f_\alpha\left(\sqrt{\frac{v}{y}}\right)\sin(\pi v)\,dv$$
$$= g_0(\alpha, y) + g_\zeta(\alpha, y),$$

where

$$g_0(\alpha, y) = \sum_{j=0}^{k-1}\int_0^1 \left(f_\alpha\left(\sqrt{\frac{v+2j}{y}}\right) - f_\alpha\left(\sqrt{\frac{v+2j+1}{y}}\right)\right)\sin(\pi v)\,dv;$$

$$g_\zeta(\alpha, y) = \int_0^{\zeta} f_\alpha\left(\sqrt{\frac{v+2k}{y}}\right)\sin(\pi v)\,dv.$$

By the support assumption on f_α, it follows that there exists at least one j with $0 \leqslant j \leqslant k-1$ such that $f_\alpha(\sqrt{\frac{2j}{\rho}}) - f_\alpha(\sqrt{\frac{2j+1}{\rho}}) > 0$. It follows that $g_0(\alpha, y) > 0$ and $g_\zeta(\alpha, y) \geqslant 0$. Hence $g(\alpha, y) > 0$. □

3.2. Proof of main theorem

We can now prove Theorem 3.1.

Proof of Theorem 3.1. Part (i) of the theorem follows directly from the localization Lemma 3.1.

Also by Lemma 3.1, in order to estimate the asymptotic decay of $\mathcal{SH}_\psi B(a, s_1, s_2, p)$, as $\alpha \to 0$, it is sufficient to examine the asymptotic decay of $I_1(a, s_1, s_2, p)$, where $p \in S$. Recall that this integral is defined only for $x \in S \cap B_\epsilon(p)$, where $\epsilon > 0$.

Without loss of generality, we may assume that $S = \{(G(u), u)\colon\ u \in U\}$, where U is a small neighborhood of $u_0 \in \mathbb{R}^2$ and $p = (G(u_0), u_0)$. We may also assume that $\nabla G(u_0) = (0, 0)$ (see remarks at the end of the proof for case $\nabla G(u_0) \neq (0, 0)$). Let $A_G(u)$ be the matrix $(G_{u_i u_j}(u_0))_{1 \leqslant i, j \leqslant 2}$ and let $K(u)$ be the Gaussian curvature of S at $(G(u), u)$, that is,

$$K(u) = \frac{\det(A_G(u))}{(1 + \|\nabla G(u)\|^2)^{\frac{3}{2}}}. \tag{9}$$

By (9) and the assumption that $K(u_0) > 0$, it follows that the matrix $A_G(u_0)$ is either positive definite or negative definite. Without loss of generality, we may assume that $A_G(u_0)$ is negative definite so that G has a local maximum at u_0 (the situation where $A_G(u_0)$ is positive definite can be treated similarly).

Using this representation for S and p, we can express $I_1(a, s_1, s_2, p)$, given by (8), as

$$I_1(a, s_1, s_2, p) = -\frac{1}{2\pi i a}\int_U J(a, s_1, s_2, p, u)\big(1 + \big\|\nabla G(u)\big\|^2\big)^{\frac{1}{2}}\,du, \tag{10}$$

where

$$J(a, s_1, s_2, p, u) = \int_0^{2\pi}\int_0^{\pi}\int_0^{\infty} \hat{\psi}_2\big(a^{-\frac{1}{2}}(\cot\phi\sec\theta - s_2)\big)\hat{\psi}_2\big(a^{-\frac{1}{2}}(\tan\theta - s_1)\big)$$
$$\times\ \hat{\psi}_1(\rho\sin\phi\cos\theta)e^{2\pi i\frac{\rho}{a}\Theta(\phi,\theta)\cdot(p-(G(u),u))}\Theta(\phi,\theta)\cdot\vec{n}(u)\rho\sin\phi\,d\rho\,d\phi\,d\theta.$$

Proof of (ii). Case $\Theta(\phi_0, \theta_0) \neq \pm\vec{n}(p)$.

Since the tangent plane of S at p is generated by the two tangent vectors $(G_{u_1}(u_0), 1, 0) = (0, 1, 0)$ and $(G_{u_2}(u_0), 0, 1) = (0, 0, 1)$ (so that $\vec{n}(p) = (1, 0, 0)$), we must have either $\Theta(\phi_0, \theta_0)\cdot(0, 1, 0) \neq 0$ or $\Theta(\phi_0, \theta_0)\cdot(0, 0, 1) \neq 0$.

Since I_1 is defined for $x \in S \cap B_\epsilon(p)$, with any $\epsilon > 0$, we can take ϵ sufficiently small and, as a consequence, U sufficiently small, so that, for all ϕ, θ, and $u \in U$, one has $\Theta(\phi,\theta)\cdot(G_{u_1}(u), 1, 0) \neq 0$ or $\Theta(\phi,\theta)\cdot(G_{u_2}(u), 0, 1) \neq 0$.

Let $Q_1(\phi,\theta) = \{u\colon\ \Theta(\phi,\theta)\cdot(G_{u_1}(u), 1, 0) \neq 0\}$ and $Q_2(\phi,\theta) = \{u\colon\ \Theta(\phi,\theta)\cdot(G_{u_2}(u), 0, 1) \neq 0\}$.

By the localization Lemma 3.1, in order to estimate I_1, we may insert a function $F(u) \in C_0^\infty(U)$ into the integral (10), with $F(u) = 1$ on a sufficiently small compact subset of U, so that for $u \in Q_j(\phi,\theta)$, $j = 1, 2$, we can integrate by parts with respect to u repeatedly. This shows that, for any positive integer N, there is a positive constant C_N such that: $|I_1(a, s_1, s_2, p)| \leqslant C_N a^N$.

Proof of (iii). Case $\Theta(\phi_0, \theta_0) = \pm\vec{n}(p)$.

Since this part of the proof is rather involved, we first give a brief outline of the arguments which will be used. As a first step, we apply the method of stationary phase (Lemma 3.2) to the integral I_1 (in formula (10)), which produces a factor a canceling the factor $\frac{1}{a}$. Our second step is to apply the change variables $t_1 = a^{-\frac{1}{2}} \tan\theta$ and $t_2 = a^{-\frac{1}{2}} \cot\phi \sec\theta$ into I_1 in order to apply Lemma 3.4. This allows us to compute the limits, as $a \to 0$, for many auxiliary functions needed to analyze I_1. In addition, since the variable u is also involved, we apply the Inverse Function Theorem to express u as a function of ϕ and θ. From all this, using the assumption of positive Gaussian curvature for the surface and Lemma 3.4, we show that $\lim_{a\to 0} a^{-1}\mathcal{SH}_\psi B(a, s_1, s_2, p)$ must have a positive real part.

Let $H_{\phi,\theta}(u) = \Theta(\phi,\theta) \cdot (p - (G(u), u))$, and $F(\phi,\theta,u) = (F_1(\phi,\theta,u), F_2(\phi,\theta,u))$, where

$$F_1(\phi,\theta,u) = \Theta(\phi,\theta) \cdot \big(G_{u_1}(u), 1, 0\big),$$
$$F_2(\phi,\theta,u) = \Theta(\phi,\theta) \cdot \big(G_{u_2}(u), 0, 1\big).$$

Since $\vec{n}(p) = (1,0,0)$ and $\Theta(\phi_0,\theta_0) = \pm\vec{n}(p)$, it follows that $\phi_0 = \frac{\pi}{2}$ and $\theta = 0$ or π. We will only consider the case $\theta_0 = 0$ since the argument for the case where $\theta_0 = \pi$ is similar.

By the assumption on $\Theta(\phi_0,\theta_0)$, it follows that $F(\phi_0,\theta_0,u_0) = (0,0)$. It is also easy to verify that the Jacobian $J_u(F)(\phi_0,\theta_0,u_0) = \det(A_G(u_0)) = K(u_0) \neq 0$. By part (i) of Lemma 3.3, it follows that there exists a smooth function $u = (u_1,u_2) = (u_1(\phi,\theta), u_2(\phi,\theta))$ in a small neighborhood J of (ϕ_0,θ_0) such that $F(\phi,\theta,u(\phi,\theta)) = (0,0)$ in J. This means that, for each fixed $(\phi,\theta) \in J$, $u(\phi,\theta) = (u_1(\phi,\theta), u_2(\phi,\theta))$ is a critical point of $H_{\phi,\theta}(u)$. Hence, from (9) we have that, for $(\phi,\theta) \in J$,

$$\det\big(A_{H_{\phi,\theta}}\big(u(\phi,\theta)\big)\big) = (\sin\phi\cos\theta)\det\big(A_G\big(u(\phi,\theta)\big)\big) = \sin\phi\cos\theta K\big(u(\phi,\theta)\big)\big(1 + \big\|\nabla G\big(u(\phi,\theta)\big)\big\|^2\big)^{\frac{3}{2}} \neq 0.$$

We notice that $\vec{n}(u(\phi,\theta)) = \Theta(\phi,\theta)$ for $(\phi,\theta) \in J$. Applying Lemma 3.2 and omitting the higher order decay term (as $a \to 0$), we have

$$\begin{aligned} I_1(a,s_1,s_2,p) = {} & \frac{i}{2\pi} \int_0^{2\pi}\int_0^{\pi}\int_0^{\infty} \hat{\psi}_1(\rho\sin\phi\cos\theta)\hat{\psi}_2\big(a^{-\frac{1}{2}}(\tan\theta - \tan\theta_0)\big) \\ & \times \hat{\psi}_2\big(a^{-\frac{1}{2}}(\cot\phi\sec\theta - \cot\phi_0\sec\theta_0)\big) e^{2\pi i \frac{\rho}{a}\Theta(\phi,\theta)\cdot(p-(G(u(\phi,\theta)),u(\phi,\theta)))} \\ & \times (\sin\phi)^{\frac{1}{2}}(\cos\theta)^{-\frac{1}{2}}\big(K\big(u(\phi,\theta)\big)\big)^{-\frac{1}{2}}\big(1 + \big\|\nabla G\big(u(\phi,\theta)\big)\big\|^2\big)^{-\frac{1}{4}}\, d\rho\, d\phi\, d\theta. \end{aligned}$$

We write this expression as

$$I_1(a,s_1,s_2,p) = Y_1(a,s_1,s_2,p) + Y_2(a,s_1,s_2,p),$$

where Y_1 corresponds to $\theta \in (-\frac{\pi}{2}, \frac{\pi}{2})$ and Y_2 corresponds to $\theta \in (\frac{\pi}{2}, \frac{3\pi}{2})$.

We start by examining the term $Y_1(a,s_1,s_2,p)$. Let $t_1 = a^{-\frac{1}{2}}(\tan\theta - \tan\theta_0) = a^{-\frac{1}{2}}\tan\theta$ and $t_2 = a^{-\frac{1}{2}}(\cot\phi\sec\theta - \cot\phi_0\sec\theta_0) = a^{-\frac{1}{2}}\cot\phi\sec\theta$. It follows that $\tan\theta = a^{\frac{1}{2}}t_1$, $\cot\phi = a^{\frac{1}{2}}t_2\cos\theta$ and, hence, $\lim_{a\to 0}\theta = 0$, $\lim_{a\to 0}\phi = \frac{\pi}{2}$. From (ii) of Lemma 3.3, a direct calculation gives that

$$\lim_{a\to 0} u_{1\phi} = -G_{u_1u_2}(u_0)K(u_0)^{-1};$$
$$\lim_{a\to 0} u_{2\phi} = -G_{u_1^2}(u_0)K(u_0)^{-1};$$
$$\lim_{a\to 0} u_{1\theta} = -G_{u_2^2}(u_0)K(u_0)^{-1};$$
$$\lim_{a\to 0} u_{2\theta} = -G_{u_1u_2}(u_0)K(u_0)^{-1}.$$

Also, it is easy to verify that $\lim_{a\to 0}\frac{\phi-\phi_0}{a^{\frac{1}{2}}} = -t_2$, $\lim_{a\to 0}\frac{\theta-\theta_0}{a^{\frac{1}{2}}} = t_1$. Omitting the higher order decay terms, we have

$$u_1(\phi,\theta) - u_1(\phi_0,\theta_0) = u_{1\phi}(\phi-\phi_0,\theta) + u_{1\theta}(\phi,\theta-\theta_0),$$
$$u_2(\phi,\theta) - u_2(\phi_0,\theta_0) = u_{2\phi}(\phi-\phi_0,\theta) + u_{2\theta}(\phi,\theta-\theta_0).$$

It follows that

$$\lim_{a\to 0}\frac{u_1(\phi_0,\theta_0) - u_1(\phi,\theta)}{a^{\frac{1}{2}}} = K(u_0)^{-1}\big(G_{u_2^2}(u_0)t_1 - G_{u_1u_2}(u_0)t_2\big);$$
$$\lim_{a\to 0}\frac{u_2(\phi_0,\theta_0) - u_2(\phi,\theta)}{a^{\frac{1}{2}}} = K(u_0)^{-1}\big(G_{u_1u_2}(u_0)t_1 - G_{u_1^2}(u_0)t_2\big).$$

Using the fact that $\nabla G(u_0) = 0$ and omitting the higher order decay terms, we have that

$$G(u) - G(u_0) = \frac{1}{2}\big(G_{u_1^2}(u_0)(u_1 - u_{01})^2 + 2G_{u_1u_2}(u_1 - u_{01})(u_2 - u_{02}) + G_{u_2^2}(u_0)(u_2 - u_{02})^2\big), \tag{11}$$

where we used the notation $u_{10} = u_1(\phi_0, \theta_0)$, $u_{20} = u_2(\phi_0, \theta_0)$. It follows that

$$\lim_{a\to 0} \frac{1}{a}\Theta(\phi, \theta) \cdot \big(p - \big(G\big(u(\phi, \theta)\big), u(\phi, \theta)\big)\big) = Q_1(t_1, t_2), \tag{12}$$

where

$$Q_1(t_1, t_2) = \frac{1}{2}\big(G_{u_1^2}(u_0)q_1^2 + 2G_{u_1u_2}(u_0)q_1q_2 + G_{u_2^2}(u_0)q_2^2\big) + q_1t_1 + q_2t_2,$$

$q_1 = K(u_0)^{-1}(G_{u_2^2}(u_0)t_1 - G_{u_1u_2}(u_0)t_2)$, $q_2 = K(u_0)^{-1}(G_{u_1u_2}(u_0)t_1 - G_{u_1^2}(u_0)t_2)$.

We finally have

$$\lim_{a\to 0} a^{-1}Y_1(a, s_1, s_2, p) = \frac{i}{\sqrt{K(u_0)}} \int_0^\infty \int_{-\frac{\sqrt{2}}{4}}^{\frac{\sqrt{2}}{4}} \int_{-\frac{\sqrt{2}}{4}}^{\frac{\sqrt{2}}{4}} \hat{\psi}_1(\rho)\hat{\psi}_2(t_1)\hat{\psi}_2(t_2)e^{2\pi i\rho Q_1(t_1,t_2)}\, dt_1\, dt_2\, d\rho. \tag{13}$$

It is easy to see that, for all ϕ near $\frac{\pi}{2}$ and θ near 0 (or, equivalently, for u near $u_0 = p$), the matrix $(A_{H_{\phi,\theta}})(u_{\phi,\theta})$ is positive definite and, hence, by the definition of $u_{\phi,\theta}$, it follows that $H_{\phi,\theta}(u)$ has a local minimum at $u_{\phi,\theta}$. Since it is clear that $H_{\phi,\theta}(u_0) = 0$, it follows that $H_{\phi,\theta}(u_{\phi,\theta}) \leqslant 0$. This implies that $Q_1(t_1, t_2) \leqslant 0$.

To examine the term Y_2, let us first apply the change of variable: $\theta \to \theta + \pi$. Then, using the same argument as for Y_1 and the assumptions that $\hat{\psi}_1$ is odd and $\hat{\psi}_2$ is even, one obtains that

$$\lim_{a\to 0} a^{-1}Y_2(a, s_1, s_2, p) = \frac{-i}{\sqrt{K(u_0)}} \int_0^\infty \int_{-\frac{\sqrt{2}}{4}}^{\frac{\sqrt{2}}{4}} \int_{-\frac{\sqrt{2}}{4}}^{\frac{\sqrt{2}}{4}} \hat{\psi}_1(\rho)\hat{\psi}_2(t_1)\hat{\psi}_2(t_2)e^{2\pi i\rho Q_2(t_1,t_2)}\, dt_1\, dt_2\, d\rho, \tag{14}$$

where $Q_2(t_1, t_2) \geqslant 0$.

For $\alpha \in [0, 2\pi)$, let $\beta_1(\alpha) = -2Q_1(\cos\alpha, \sin\alpha)$ and $\beta_2(\alpha) = 2Q_2(\cos\alpha, \sin\alpha)$. It follows that $\beta_1(\alpha) \geqslant 0$ and, for some α, $\beta_1(\alpha) > 0$. Similarly, we have that $\beta_2(\alpha) \geqslant 0$ and, for some α, $\beta_2(\alpha) > 0$. Combining (13) and (14) and applying Lemma 3.4, we conclude that

$$\begin{aligned}
\Re\Big(\lim_{a\to 0} a^{-1}\mathcal{SH}_\psi B(a, s_1, s_2, p)\Big) &= \Re\Big(\lim_{a\to 0} a^{-1}\big(Y_1(a, s_1, s_2, p) + Y_2(a, s_1, s_2, p)\big)\Big) \\
&= \frac{1}{\sqrt{K(u_0)}} \int_0^\infty \hat{\psi}_1(\rho) \int_0^{2\pi}\int_0^1 \hat{\psi}_2(r\cos\alpha)\hat{\psi}_2(r\sin\alpha) \\
&\quad \times \big(\sin\big(\pi\beta_1\rho r^2\big) + \sin\big(\pi\beta_2\rho r^2\big)\big) r\, dr\, d\alpha\, d\rho > 0.
\end{aligned}$$

This completes the proof of part (iii). □

Remarks about the proof

- At the beginning of the proof, we assumed $\nabla G(u_0) = (0, 0)$ so that $\Theta(\phi_0, \theta_0) = \vec{n}_p = (1, 0, 0)$. If $\nabla G(u_0) \neq (0, 0)$, then we still have $\Theta(\phi_0, \theta_0) = \vec{n}_p$. Then the proof proceeds in essentially the same way, up the following two minor differences. First, in the proof of part (iii), using expression (9), $J_u(F)(\phi_0, \theta_0, u_0) = \det(A_G(u_0)) = K(u_0)$ is replaced by $J_u(F)(\phi_0, \theta_0, u_0) = \det(A_G(u_0)) = cK(u_0)$ for $c > 0$. This has no effect on the rest of the argument. The other difference is in Eq. (11), where an additional term involving a $\nabla G(u_0)$ factor must be added to the sum. However, since $\Theta(\phi_0, \theta_0) \cdot (G_{u_1}(u_0), 1, 0) = 0$ and $\Theta(\phi_0, \theta_0) \cdot (G_{u_2}(u_0), 0, 1) = 0$, one can verify that Eq. (12) still holds with a slightly different $Q_1(t_1, t_2)$ (but still homogeneous of degree 2 with respect to (t_1, t_2)) and the rest of the argument is the same.
- In the proof, we assumed that the surface is parametrized as $(G(y, z), y, z)$, for $(y, z) \in U$, where U is a small neighborhood of $(0, 0)$. In this situation, for $(y, z) \in U$ there is an $s = (s_1, s_2)$ which corresponds to the normal orientation and this was considered in our argument. This parametrization covers the most general case for the horizontal shearlet system we are considering here. For a different parametrization such as the surface $(x, y, G(x, y))$, $(x, y) \in U$, it is possible that there is no $s = (s_1, s_2)$ which corresponds to the normal orientation. In this case, the proof is significantly simplified since one only needs to prove parts (i) and (ii).

3.3. Comments and extensions

It is interesting to observe that the asymptotic behavior of the continuous shearlet transform found at the beginning of Section 3 for the discontinuity along a plane is consistent with Theorem 3.1; in both cases the asymptotic decay rate is rapid for all locations and orientations except at the singularity locations, for normal orientations, where the asymptotic decay rate is $O(a^{-1})$. However, the arguments used to prove the two cases are very different and not interchangeable. In the case of a plane-discontinuity, the proof follows directly from the computation of the Fourier transform of a distribution. This is similar to arguments used in [1,11] and can be generalized to deal with more general regions bounded by planes using appropriate localization results as those developed in [6]. Conversely, the approach of Theorem 3.1, which is much more involved, does not require the explicit computation of the Fourier transform of the function to be analyzed, but this function is required have compact support and satisfy certain regularity assumptions.

It is natural to ask how the results presented in this work extend to situations where

- the function $B = \chi_\Omega$ is replaced by a more general compactly supported function;
- the boundary surface $\partial\Omega$ contains irregular points such as cusps or wedges.

Unfortunately, in both cases, these extensions are significantly more complicated than the 2D case, and cannot be carried over using directly the ideas from the 2D case from the 3D method introduced above.

Specifically, in dimension $n = 2$, it is shown in [7] that the function $B = \chi_D$, where D is a bounded planar region with smooth boundary, can be replaced by a smooth compactly supported function f in the following way. Let p be any point on the boundary of D with $f(p) \neq 0$. Then one can replace $B = \chi_D$ with $f\chi_D$ at p and show that the asymptotic decay rate for the error term $(f - f(p))\chi_D$, as $a \to 0$, is faster than $a^{3/4}$. Indeed a similar result holds in dimension $n = 3$. However, when $f(p) = 0$, then one has to use $Pf(p)\chi_D$ to replace $f\chi_D$ near p, where $Pf(p)$ is a suitable Taylor polynomial of f at p. The estimates for the error term is still valid and one can still control the upper bound for $Pf(p)\chi_D$. The problem is that now one cannot use the same idea as dimension $n = 2$ to control lower bound for $Pf(p)\chi_D$ since Lemma 3.4 (the analog of Lemma 4.4 in [7] for dimension $n = 2$) is not useful to deal with this case.

Finally, concerning the applicability of these results to discrete applications such as 3D edge detection, it is clear that asymptotic estimates like those provided in Theorem 3.1 do not lead directly to efficient numerical algorithms. In dimension $n = 2$, this issue was addressed by the authors and their collaborators in [16,17] where it was discussed how to apply these types of theoretical results to obtain effective algorithms for edge analysis and detection. The extension of these discrete applications to 3D is currently under investigation.

References

[1] E.J. Candès, D.L. Donoho, Continuous curvelet transform: I. Resolution of the wavefront set, Appl. Comput. Harmon. Anal. 19 (2005) 162–197.
[2] S. Dahlke, G. Steidl, G. Teschke, The continuous shearlet transform in arbitrary dimensions, J. Fourier Anal. Appl. 16 (3) (2010) 340–364.
[3] G. Easley, D. Labate, W. Lim, Sparse directional image representations using the discrete shearlet transform, Appl. Comput. Harmon. Anal. 25 (2008) 25–46.
[4] K. Guo, G. Kutyniok, D. Labate, Sparse multidimensional representations using anisotropic dilation and shear operators, in: G. Chen, M. Lai (Eds.), Wavelets and Splines, Nashboro Press, Nashville, TN, 2006, pp. 189–201.
[5] K. Guo, D. Labate, Optimally sparse multidimensional representation using shearlets, SIAM J. Math. Anal. 39 (2007) 298–318.
[6] K. Guo, D. Labate, Characterization and analysis of edges using the continuous shearlet transform, SIAM J. Imaging Sci. 2 (3) (2009) 959–986.
[7] K. Guo, D. Labate, W. Lim, Edge analysis and identification using the continuous shearlet transform, Appl. Comput. Harmon. Anal. 27 (1) (2009) 24–46.
[8] C.S. Herz, Fourier transforms related to convex sets, Ann. of Math. 75 (1962) 81–92.
[9] M. Holschneider, Wavelets. Analysis Tool, Oxford University Press, Oxford, 1995.
[10] L. Hörmander, The Analysis of Linear Partial Differential Operators. I. Distribution Theory and Fourier Analysis, Springer-Verlag, Berlin, 2003.
[11] G. Kutyniok, D. Labate, Resolution of the wavefront set using continuous shearlets, Trans. Amer. Math. Soc. 361 (2009) 2719–2754.
[12] G. Kutyniok, M. Shahram, D.L. Donoho, Development of a digital shearlet transform based on pseudo-polar FFT, in: Wavelets XIII, San Diego, CA, 2009, in: SPIE Proc., vol. 7446, SPIE, Bellingham, WA, 2009.
[13] Y. Meyer, Wavelets and Operators, Cambridge Stud. Adv. Math., vol. 37, Cambridge Univ. Press, Cambridge, UK, 1992.
[14] C.D. Sogge, Fourier Integrals in Classical Analysis, Cambridge Univ. Press, Cambridge, 1993.
[15] E.M. Stein, Harmonic Analysis: Real-Variable Methods, Orthogonality, and Oscillatory Integrals, Princeton University Press, Princeton, NJ, 1993.
[16] S. Yi, D. Labate, G.R. Easley, H. Krim, Edge detection and processing using shearlets, in: Proceedings IEEE ICIP, San Diego, October 12–15, 2008.
[17] S. Yi, D. Labate, G.R. Easley, H. Krim, A shearlet approach to edge analysis and detection, IEEE Trans. Image Process. 18 (5) (2009) 929–941.